

APPLICABILITY OF MAGNETIC FIELD FOR DIRECTED ORIENTATION OF STEEL FIBRES IN HIGH-PERFORMING CEMENTITIOUS COMPOSITES

KRISTÝNA TAKÁČOVÁ¹, KAREL KÜNZEL², VÁCLAV PAPEŽ², PETR KONRÁD¹, MICHAL MÁRA¹, JINDŘICH FORNŮSEK¹, PŘEMYSL KHEML¹ & RADOSLAV SOVJÁK¹

¹ Experimental Centre, Faculty of Civil Engineering, Czech Technical University in Prague, Czech Republic.

² Department of Electrotechnology, Faculty of Electrical Engineering, Czech Technical University in Prague, Czech Republic.

ABSTRACT

This paper explores the practical possibility of using a magnetic field to orient steel fibres in a fresh concrete matrix. This process leads to preferential orientation, which increases the desired mechanical properties of the hardened material. In general, this paper focuses on the technical aspects of the orientation process and identifies key areas, such as the strength and shape of the magnetic field, velocity of the sample's passage through the magnetic field and viscosity of the materials. A prototype orienting apparatus was constructed with different permanent magnet systems to evaluate their performance. An ultrasound gel and a cementitious matrix were used as a medium for the fibres. Numerical simulations were created to further understand the effects of the magnetic field's strength and shape. The final orientation of the fibres in hardened concrete was evaluated using Q factor measurements, X-ray scans and bending tests. A sufficiently strong magnetic field can be used to orient fibres in fresh concrete.

Keywords: cementitious composite, concrete, fibre orientation, HPFRC, magnetic field, steel fibre.

1 INTRODUCTION

High-performance concrete (HPC) is a material that offers many advantages compared with normal strength concrete, such as better resistance against water penetration, increased toughness, fatigue performance and subsequent longevity. However, its main disadvantage is still the brittle behaviour [1, 2]. This can be improved by adding reinforcing fibres. The resulting composite can then offer better strengths and resistance to extreme loads [3, 4]. The fibres are usually added during the mixing process, so their distribution and orientation are not directly controlled. It is also influenced by other factors such as the mould shape, workability and flow of the fresh mixture and the placement methods [5–8]. The homogeneity of the material is not automatically assured. On the contrary, the mechanical parameters of the hardened fibre-reinforced concrete can vary significantly.

This paper explores the possibility of orienting the ferromagnetic (steel) fibres embedded in a HPC matrix using a magnetic field. The general goal is to orient the fibres for maximum efficiency in terms of the expected directions of tensile stresses in the material. Ideally, fibres in the matrix need to be perpendicular to the formed cracks. This should lead to either improving the performance of the material or lowering the necessary amount of expensive reinforcing fibres in order to meet certain mechanical characteristics.

The process of orienting the fibres using a magnetic field has several technical parameters that need to be tested for their significance on the resulting orientation. These are mainly the strength of the magnetic field and the shape and direction of the magnetic field lines.

Another parameter would be the viscosity of the mixture, which is tied to the strength of the field. The field must be strong enough to overcome the resistance of the matrix. The time the material spends in the magnetic field will also be important, which will be the velocity of the movement of the sample through the magnetic field. This paper is an extended version of a conference paper [9].

2 EXPERIMENTAL PROGRAM

2.1 Materials

Two materials were chosen as a medium for the fibres – an HPC and an ultrasound gel. Mixture design of this concrete is given in Table 1. All constituents, except fibres and water, were prepared in advance in a commercial mixing facility and made into a ready-to-use bagged dry mixture. No special curing regimes were used. Samples were placed in a closed box with high relative humidity for at least 28 days after manufacturing. This mixture design was chosen as it was readily available, it offered suitable rheological properties and the authors already had extensive experience with it. The ultrasound gel was chosen primarily because of its transparency so that the fibre orientation can be observed directly. When mixed with water (1 part gel to 0.566 part water), it achieves similar rheological properties as the concrete (confirmed in [10]). Several other gel-to-water ratios were used to test different viscosities which will be further explained together with the results. The viscosity was measured using a rotational viscometer Brookfield DV-II+Pro on fibre-free samples. Fibres were straight steel 13 mm long with a diameter of 0.14 mm and tensile strength of 2800 MPa (stated by the manufacturer). Volumetric content of fibres was 1.5 % for all experiments with the ultrasound gel and 1.5 % and 0.75 % for the concrete. The ultrasound gel samples had dimensions of 45 × 23 × 75 mm, and the concrete samples had dimensions of 40 × 40 × 160 mm.

2.2 Methods and measurements

2.2.1 Ferrite rings with neodymium magnets

Figure 1 shows the prototype mechanism, which forms a track for the sample's tray. The tray is connected to a drive screw, which is rotated by a small electric motor. Varying the voltage applied to the motor allows for variable tray velocity as it passes through the magnetic field. All parts of the structure are made of wood or plastic to not react to the magnetic field. In

Table 1: Material constituents relative to the cement content and water dosage [11].

Cement	1
Silica fume	0.10
Silica powder	0.25
Silica sand 0.1–1.2 mm	1.60
High range water reducer	0.01
Anti-foaming agent	0.001
Water (dry mixture's weight)	10 %

this case, the magnetic field is created using ferrite rings and neodymium (NdFeB) magnets. A schematic of this configuration can be seen in Fig. 2. The ferrite rings had 140 mm outer, 64 mm inner diameters and 17 mm thickness and were made from CF 139 material. The neodymium magnets had dimensions of $42 \times 20 \times 10$ mm and were made from N38 material. Ferrite, in this case, acts as a good magnetic field conductor. In combination with the stronger neodymium magnets, the whole systems act as a strong ring magnet. Ferrite magnets are generally more readily available in these kinds of shapes, compared to more expensive neodymium magnets that would have to be custom-ordered.

Strength of the magnetic field could have been altered by adding or removing the neodymium magnets. Permanent magnets were used for their simplicity, lack of power supply and durability. A major disadvantage of this solution is that the sample size is limited by the ferrite ring's inner diameter. A ruler is positioned on the side of the track. Each passage of the tray is recorded on a camera so that the ruler is visible. The tray's velocity can be calculated this way.

2.2.2 C-shaped ferrite core with neodymium magnets

The second configuration, and all subsequent configurations, used the same prototype of the basic structure but employed a different system of magnets. The aim of this design was to eliminate the sample size constraint. Figure 3 shows that C-shaped ferrite cores with neodymium magnets were used and placed on the side of the track. This would have allowed for practically any sample geometry to be placed between the magnets since the free space

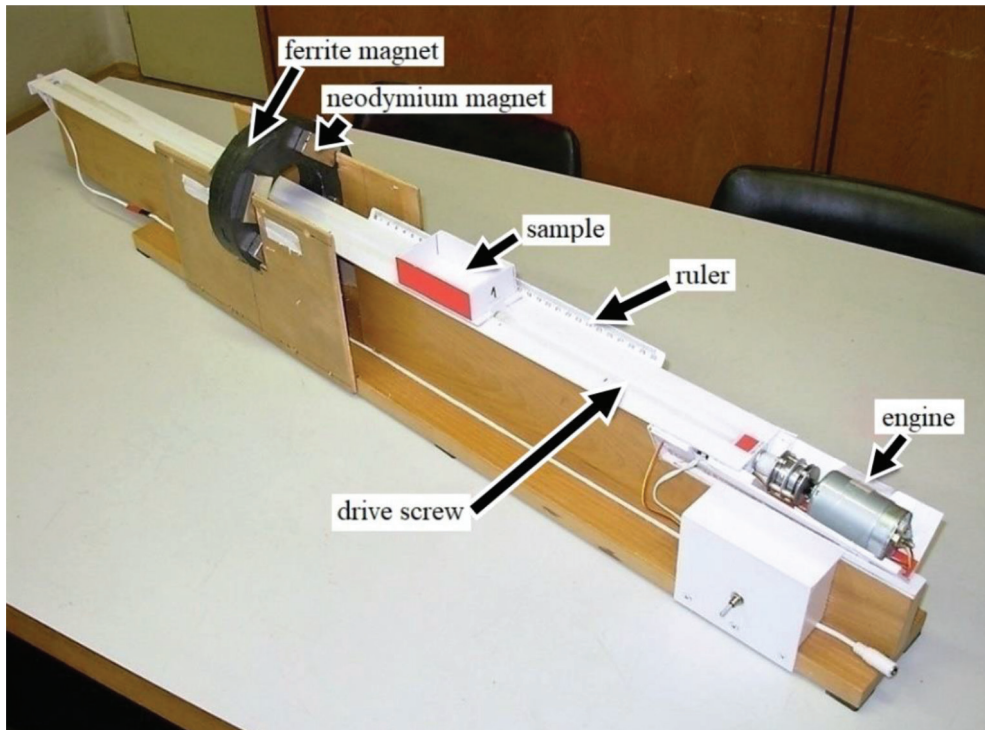


Figure 1: Prototype of the fibre-orienting mechanism with the ferrite rings magnet configuration.

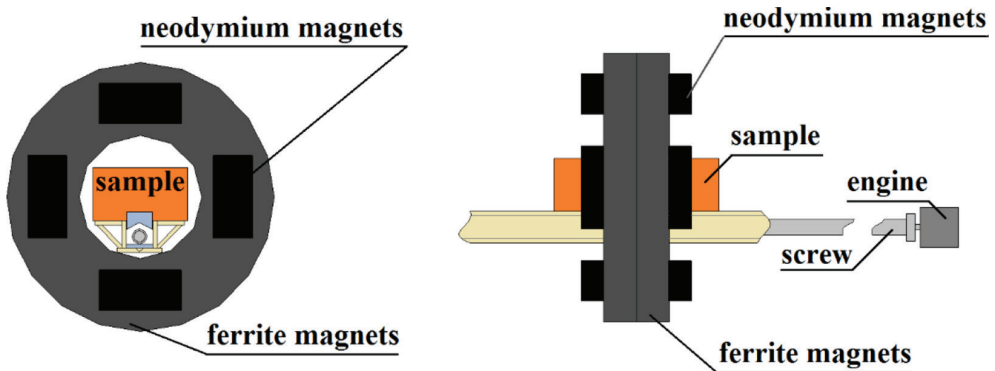


Figure 2: Detailed schematic of the configuration of the ferrite rings and neodymium magnets.

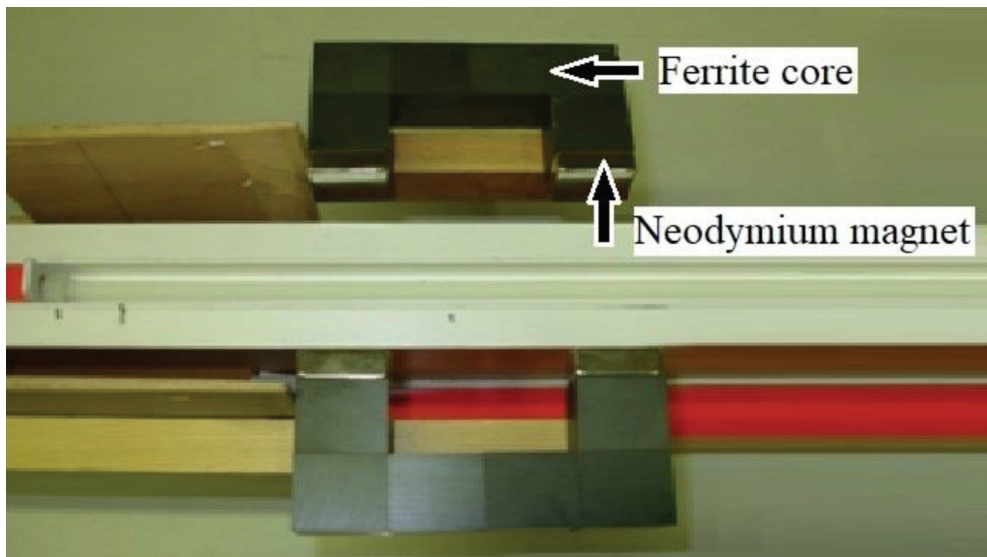


Figure 3: The C-shaped ferrite core with neodymium magnets configuration.

between them is not limited by the magnet size. The C-shaped core was made of ferrite cubes with dimensions of $25 \times 25 \times 25$ mm. The neodymium magnets were $25 \times 25 \times 10$ mm large. Both magnet types were made from the same material as described in Section 2.2.1.

2.2.3 In-line ferrite core with neodymium magnets

Similarly to the second option, the third configuration also used two separate magnet systems on the side of the tracks. Figure 4 shows this third design. One part consists of three ferrite cubes with additional neodymium magnets on the ends. These are the same magnets as used before.

2.2.4 Evaluating the fibre orientation

Due to the transparency of the ultrasound gel, the fibre orientation can be evaluated visually. However, more complicated methods need to be used for the concrete. In this research, two possible techniques were used. Samples have been scanned using an X-ray diagnostic

machine. This scanning provided pictures from which a 3D model of the scanned area was reconstructed. The models could then be, again, visually evaluated, as the fibre orientation was apparent. On the other hand, the X-ray scanning is relatively expensive, the sample size is limited and the scanning and subsequent analysis is significantly time-consuming.

The second technique is the measurement of the quality factor Q , which is a parameter of an electrical coil that depends on its shape, the number of wire turns, wire diameter, wire material, coil core, voltage and current to be supplied and its frequency. The quality factor Q was measured using an impedance meter (Agilent E4991A). Measurements were made using 27 coil turns made of copper wire with a diameter of 1.8 mm and with a frequency ranging from 1 to 3 MHz. The coil was square-shaped so the samples would fit tightly inside of it.

The quality factor Q can be expressed as

$$Q = \frac{R}{X_L} \quad (1)$$

where R (Ω) is resistance and X_L (Ω) is inductive reactance. Higher values of the quality factor express a better ratio of inductance as the main required property to undesired losses represented by ohmic resistance. A single layer air coil with high-quality factor is used. Inserting a sample containing ferromagnetic fibres will change the inductance of the coil as well as the losses in the coil. The losses are caused mainly by hysteresis losses of the used material. Measurements are performed at frequencies where losses in ferromagnetic fibres are maximised. It has been presumed that samples with a larger number of oriented fibres,

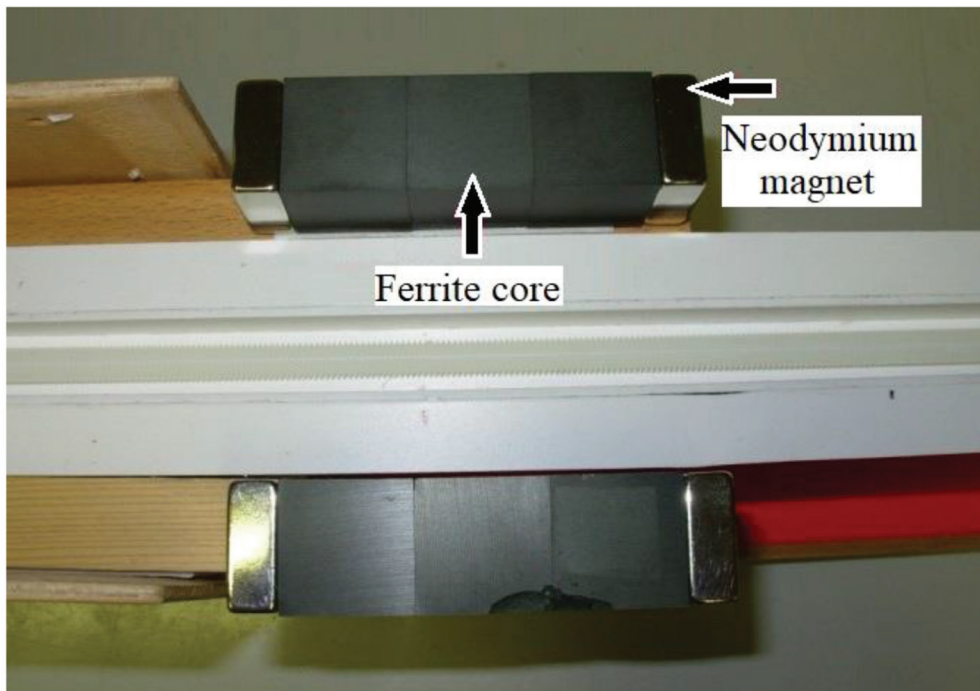


Figure 4: The in-line ferrite core with neodymium magnets configuration.

or with fibres oriented more parallel to the coil axis, will allow better magnetisation of fibres accompanied by higher losses. Oriented fibre samples will show a significant decrease in the quality factor Q . The measurement has a comparative character. It allows to compare samples with the same fibre content and different orientation or to compare the same oriented samples with different fibre content.

The samples were placed inside the measuring coil so they formed a rod core. The coil core, i.e. the concrete sample with steel fibres, was monitored during the measurement to determine the coil quality factor. It has been confirmed that the coil quality factor decreases with the desired orientation of the fibres. It has also been verified that the permeability of plain concrete or plain ultrasound gel is practically the same as the permeability of the air. This means that the quality factor will not change significantly with the placement of the plain concrete or ultrasound gel into the coil.

3 INVESTIGATION OF THE INFLUENCE OF THE MAGNETIC FIELD ON THE FIBRE

Calculating the intensity of the magnetic field of a system of permanent magnets or a wound coil and calculating the force effects on an inserted ferromagnetic fibre is not a trivial problem. Although in some cases the arrangement can be simplified to a 2D problem, concerning the assumed further solution of the interaction of two or more fibres, it can be a problem in 3D. To solve the shape of the magnetic field and its force effects, we can use the finite element method. For these purposes, many software packages are available that focus on a variety of technical issues, including the investigation of the properties of the electromagnetic field. Mathematically, the solution is based on Maxwell's equations describing the electromagnetic field. Continuous space is then replaced by discrete points in which we investigate specific physical quantities following the equations. These points form a so-called mesh. With a suitable choice of the mesh and its sufficient resolution, we can then obtain a result that is close to the continuous solution with adequate accuracy.

Our goal was to investigate the shape of the magnetic field and the intensity of the magnetic field near a given system of permanent magnets with a defined remanent magnetic induction. A structural steel fibre with a defined magnetisation characteristic was placed in the magnetic field. The intensities of the magnetic field around the fibre were calculated. Another calculated quantity was the moment acting on the fibre.

ANSYS Workbench using magnetostatic systems analysis was chosen as a suitable software package. An example of the arrangement of permanent magnets described in the previous chapter after conversion to ANSYS DesignModeler is shown in Fig. 5. The examined fibre is located in the centre. Figure 6 illustrates the course of the magnetic field lines. Different colours represent different magnetic field strengths according to the scale on the left of the image. In the middle, the compaction of the lines of force is visible, as the magnetic flux is closed in an easier way, i.e. by the magnetically well-conducting material of the inserted fibre. The detail of the field around the fibre can be seen in the upper right corner. The ferromagnetic material is saturated, i.e. the magnetic induction in the fibre is practically at its maximum value and in such a state, the fibre behaves almost as a permanent magnet inserted into a magnetic field. The torque acting on the fibre in the magnetic field is investigated against a coordinate system located in the centre of the monitored fibre. We can thus determine the moment acting on the fibre depending on the angle by which the fibre is rotated to the direction of the magnetic field lines.

A comparison between various magnet systems, as described above, can be made. Figure 6 shows that the magnetic field created by the ring configuration will tend to orient the fibres parallel to the trajectory of the sample through the field. This is the desired shape of the magnetic field. Even closer to the inner diameter of the ring, the field is still mostly oriented the same way. Figure 7 shows the simulated results for the other two configurations. In this case, the shape of the magnetic field is correct between the magnets. However, closer towards the magnets it changes to be more perpendicular to the sample's trajectory. This could lead to different fibre orientation in different parts of the specimen, which is not desired.

4 RESULTS AND DISCUSSION

4.1 Fibre behaviour

In general, when a steel fibre is subjected to a magnetic field, it becomes magnetised and exhibits limited magnetic behaviour. The fibre will have residual remanence. A standard gauss meter was used to measure magnetic induction near a cluster of fibres (outside of the medium). A magnetic field of 0.04 mT was measured, which might be considered to be negligible. After exposing these fibres to a magnetic field of 44 mT, the induction was measured to be 1.16 mT, which confirms the remanence behaviour of fibres. However, this value is still small. This effect can lead to clustering or chaining of the fibres, as they would be pulled towards each other. In all of the experiments, this behaviour was not observed, as the viscous mediums prevented it. However, it is an effect that should be noted.

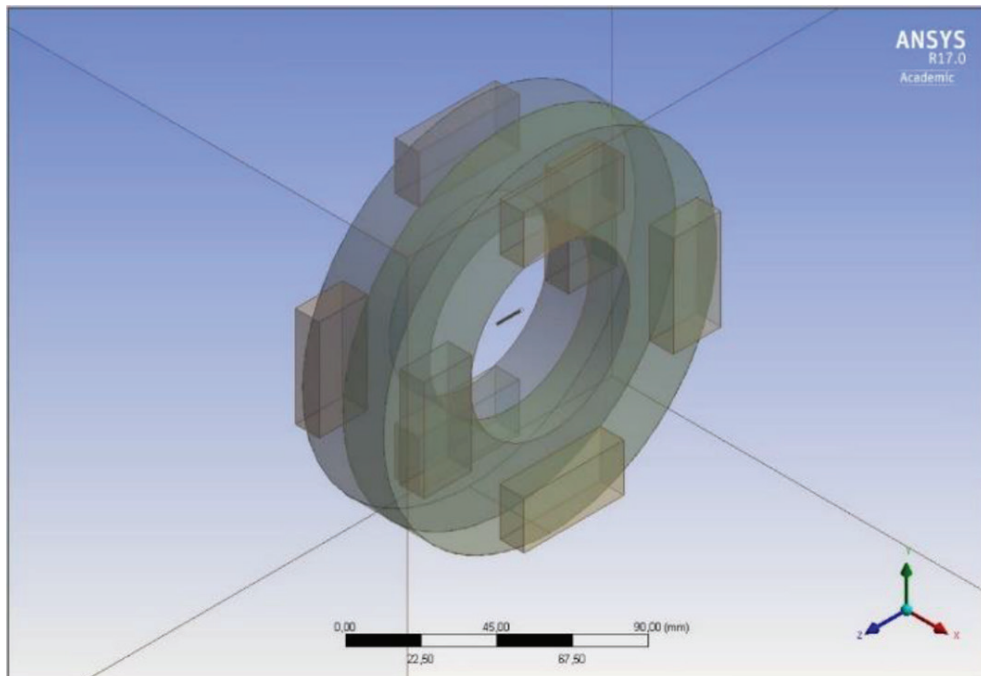


Figure 5: System of permanent magnets with inserted fibre in ANSYS DesignModeler.

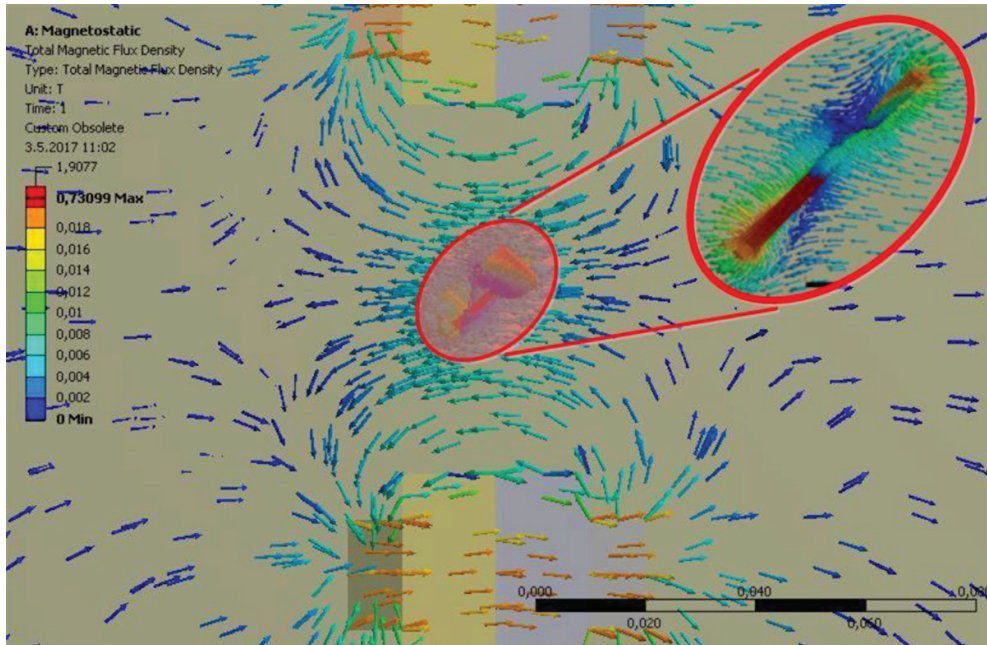


Figure 6: Simulation of effect of the magnetic field on the fibre in ANSYS. Ferrite rings with neodymium magnets.

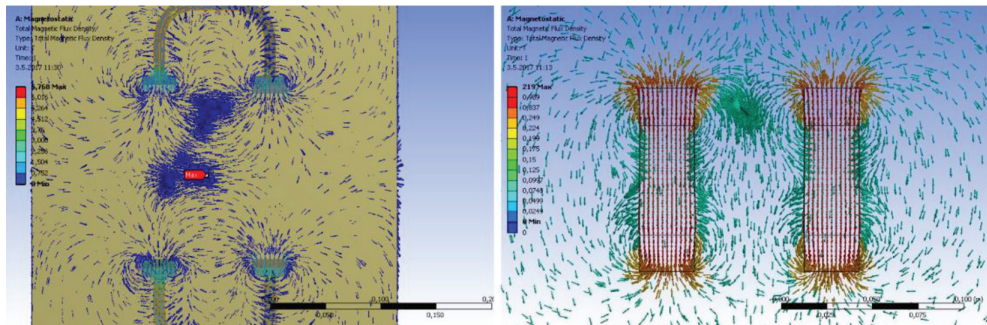


Figure 7: Simulations of the C-shaped and in-line configurations.

4.2 Ultrasound gel

The shape and strength of the magnetic field were confirmed using the ultrasound gel with fibres for all of the magnet configurations outlined in Sections 2.2.1, 2.2.2 and 2.2.3. The C-shaped and in-line systems did not result in good fibre orientation. Fibres near the edges of the tray (closest to the magnets) were partially oriented perpendicularly to the walls, while the fibres near the centre achieved limited parallel orientation. This is illustrated in Fig. 8. This confirmed the numerical simulation findings. For future testing, both of these magnet systems were abandoned.

The better orientation of fibres was achieved using the ferrite rings with neodymium magnets. This principle was used for more extensive experimental evaluation. Table 2 summarises

the testing parameters. An orientation mark was given to each of the samples. Mark 1 was the best visual orientation when the vast majority of fibres were not angled more than 30° from the longitudinal axis. Mark 5 corresponds to no visible change in fibre orientation compared to the situation before the sample passed through the magnetic field. An example of ideally oriented fibres in a sample can be seen in Fig. 9.

Four different series of ultrasound gel samples were made. The 1 to 0.556 ratio was the reference mixture, which resembled the concrete the most in terms of the rheological properties, as outlined earlier. The viscosities in Table 2 are given relative to this mixture. The viscometer used for measurements only allows comparative measurements. Therefore, exact values of viscosity are intentionally not provided, as they cannot be directly compared to other viscosity measurement methods. The field intensity value of 30 mT was the case for ferrite rings without the neodymium magnets. Adding the neodymium magnets increased the magnetic field intensity up to 55 mT with eight additional magnets. The results were otherwise as expected. Higher viscosity, lower magnetic field intensity and faster passage of the sample through the magnetic field resulted in worse orientation. For the reference mixture, the maximum magnetic field intensity together with a minimum of 20 mm/s passage velocity was required for an ideal fibre orientation.

4.3 Concrete

Concrete specimens were tested only with the ferrite rings with neodymium magnets method, as all the other methods proved unsuitable by the simulations and the ultrasound gel experiments. To further increase the strength of the magnetic field, more neodymium magnets were added, so a total of 16 neodymium magnets were used, which was a physical maximum that fits on the ferrite rings (eight on one side). This configuration produced a magnetic field



Figure 8: Unwanted fibre orientation as a result of the C-shaped and in-line magnets configuration.

Table 2: Experimental parameters and the results of the ultrasound gel testing.

Series	Ultrasound gel:water	Viscosity (-)	Field intensity (mT)	Velocity (mm/s)	Orientation mark
1	1:0	1.22	55	20	1
			55	33	1
			30	40	4–5
			55	100	1
2	1:0.556	1.00	55	20	1
			30	20	3–4
			45	20	3
			55	33	1
			55	27	2
3	1:0.35	1.03	55	20	1
			55	40	3
			55	20	2
			55	40	2–3
4	1:0.15	1.03	55	20	1
			55	20	1–2
			55	20	1



Figure 9: An ideal orientation using the ferrite rings with neodymium magnets configuration. Before and after the orientation process. Comparison of the same sample.

induction of 60 mT. Right after mixing, the fresh concrete was poured into the tray of the orienting mechanism and passed through the magnetic field at the velocity of 20 mm/s. This velocity was chosen based on the ultrasound gel results.

Figure 10 shows the results of the Q factor testing. Letter N symbolises the non-oriented samples and O refers to the samples that passed through the magnetic field. The differences between the Q factor values are apparent and were, as expected, decreasing with the number of fibres and their preferred orientation. The differences between the samples' Q factors were mostly constant across the entire frequency spectrum used for the measurements. It can also be seen that the difference between oriented and non-oriented samples was higher for the lower percentage. This might indicate a more difficult orientation of higher volumes of fibres as the individual fibre's movement was limited. The Q factors were measured in the centres of the specimens.

Figure 11 shows the load-displacement diagrams for samples tested using a three-point bending experiment (100 mm span, deformation controlled at 0.2 mm/min). Table 3 summarises these diagrams together with the maximum Q factor value measured for the respective samples. The dissipated energy was calculated as the area under the load-displacement curve up to the deflection of 3 mm. The values in brackets are the mechanical parameters relative to the non-oriented samples of the respective fibre volume. The flexural strengths and dissipated energies were further apart for the higher percentage. The dissipated energies had lower relative differences compared to the flexural strengths, as the force in the strain-softening region decayed faster after reaching higher peak forces. However, this behaviour should be expected, as all the samples used fibres of the same length. This means that ultimately, the diagrams for all fibre percentages needed to reach similar endpoints. Samples with oriented fibres did not experience sudden unstable drops in the loading force, which was probably directly caused by the preferred orientation. Even though the absolute difference for the Q factor values is higher for the lower percentage, the relative difference is not. However, the relative difference is similar for both percentages, while the increase in mechanical parameters is more significant for the higher percentage.

Figures 12 and 13 show the final 3D models reconstructed from the X-ray images. Samples on the left did not pass through the magnetic field and on the right samples that did. The fibre

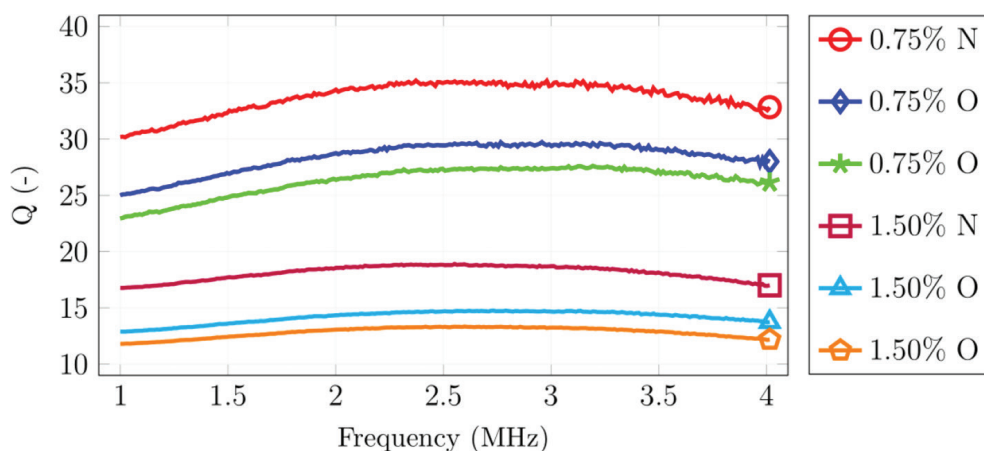


Figure 10: Measurements of the Q factor with various frequencies for the oriented (O) and non-oriented (N) samples.

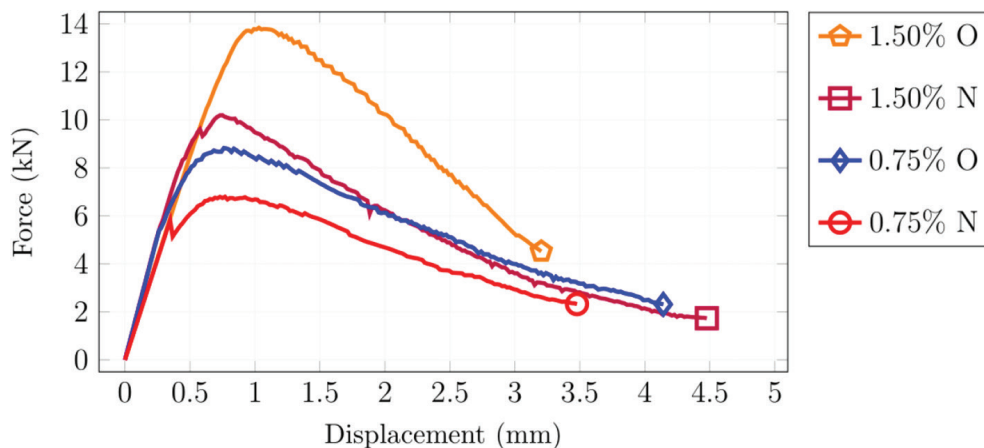


Figure 11: Load-displacement diagrams for the oriented (O) and non-oriented (N) samples.

Table 3: Summary of the experimental results.

Sample	Flexural strength (MPa)	Dissipated energy (J)	Q (-)
1.50 % O	35.30 (1.52)	28.19 (1.40)	13.34 (0.73)
1.50 % N	23.20 (1.00)	20.13 (1.00)	18.17 (1.00)
0.75 % O	20.50 (1.32)	19.02 (1.29)	27.62 (0.78)
0.75 % N	15.50 (1.00)	14.75 (1.00)	35.21 (1.00)

orientation difference is clearly visible. These images show a volume of $40 \times 40 \times 40$ mm in the centre of the 160-mm-long specimen, as that was the maximum scanning volume of the X-ray device. Due to the visual artefacts in the reconstructed model, the fibres appear thicker than they actually are, especially when not aligned vertically.

5 SUMMARY AND CONCLUSIONS

This paper focused on the possibility of controlling the orientation of steel fibres in concrete and confirming this possibility with the use of an ultrasound gel and numerical simulations. The main points of this research can be summarised as follows.

- The orientation of fibres is not only possible but also relatively simple to achieve using the special orienting device.
- Several configurations of permanent magnets were tested. Numerical simulations in ANSYS were used to evaluate the magnetic fields. The ideal shape and sufficient strength were achieved with the ring magnet configuration. This was also confirmed using the ultrasound gel experiments.
- Factors that influence the fibre orientation are the strength of the magnetic field, the shape of the magnetic field, the viscosity of the medium and velocity of the sample's passage through the magnetic field.

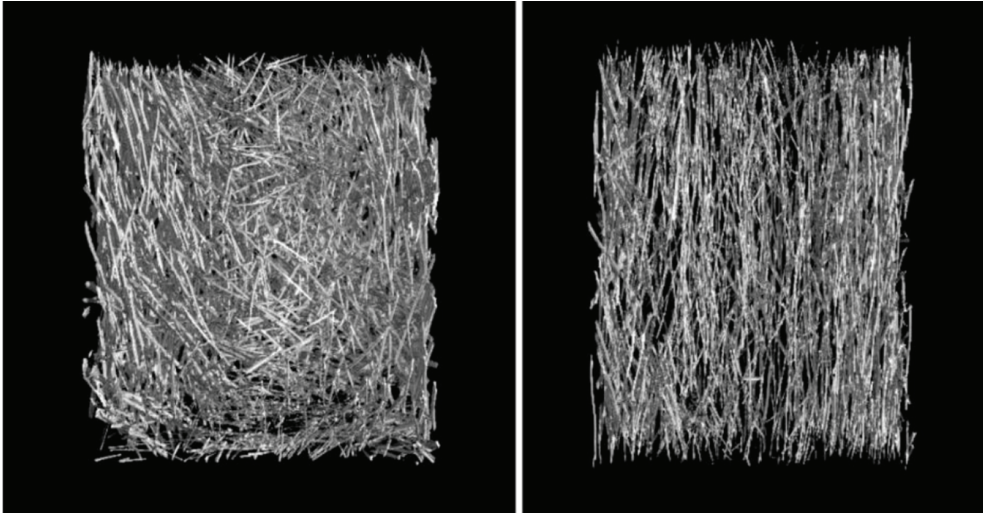


Figure 12: The 3D models of 1.5 % fibre volume samples. Left, non-oriented; right, oriented.

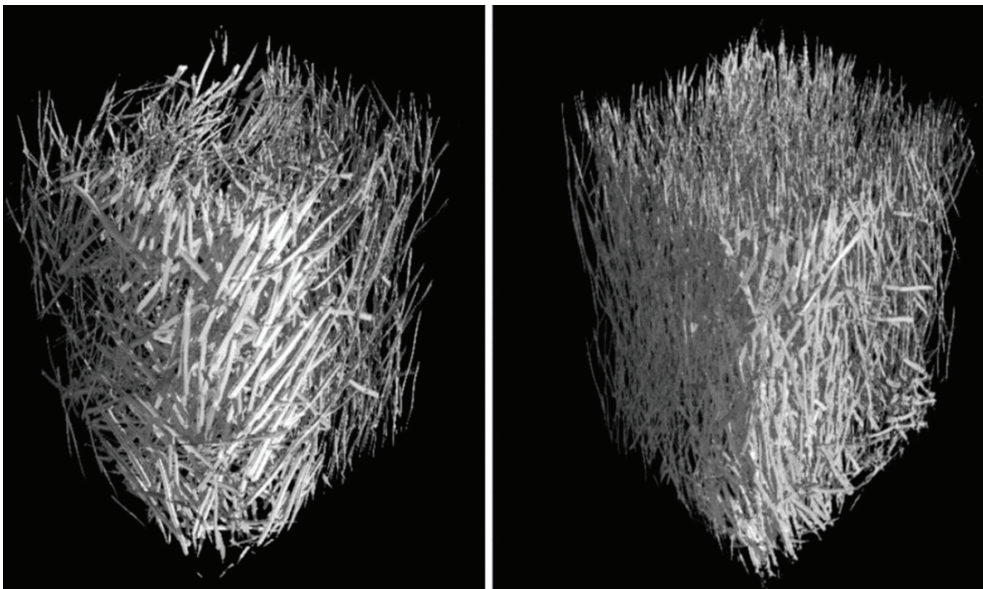


Figure 13: The 3D models of 0.75 % fibre volume samples. Left, non-oriented; right, oriented.

- The successful orientation of fibres in concrete samples was confirmed using the Q factor measurements, three-point bending experiments and X-ray scanning. The flexural strength increased by 52% and 32% for the higher and lower fibre volume, respectively.

It should be noted that the process of fibre orientation will inevitably improve the tensile properties of the material in one direction at the expense of the remaining axes. This might be counterproductive in certain applications where significant tensile stresses are expected in all axes. However, the assumption that before the directed orientation all fibres were oriented randomly, and therefore provided even reinforcement, is wrong due to the nature of manufacturing fibre-reinforced concrete. Using this method, at least one of the axes can achieve controllable fibre orientation and reinforcement. Nevertheless, it is beyond the scope of this paper to present specific applications, but it could be expected that a method of controlling the fibre orientation should benefit especially (ultra) HPC used in thin structures, small columns or beams and protective elements.

ACKNOWLEDGEMENTS

The authors gratefully acknowledge the financial support from the Czech Science Foundation (grant number GA20-00624S). The authors also acknowledge assistance from students and technical staff at the Experimental Centre of the CTU who participated on the internal CTU projects SGS19/143/OHK1/3T/11 and SGS20/054/OHK1/1T/11.

REFERENCES

- [1] Afroughsabet, V., Biolzi, L. & Ozbakkaloglu, T., High-performance fiber-reinforced concrete: A review. *J Mater Sci*, **51**(14), pp. 6517–51, 2016 July 30. <https://doi.org/10.1007/s10853-016-9917-4>
- [2] Yoo, D.-Y.D.Y. & Banthia, N., Mechanical properties of ultra-high-performance fiber-reinforced concrete: A review. *Cem Concr Compos*, **73**, pp. 267–280, 2016 October. <https://doi.org/10.1016/j.cemconcomp.2016.08.001>
- [3] Nicolaidis, D., Kanellopoulos, A., Savva, P. & Petrou, M., Experimental field investigation of impact and blast load resistance of Ultra High Performance Fibre Reinforced Cementitious Composites (UHPFRCCs). *Constr Build Mater*, **95**, pp. 566–574, 2015 October. <https://doi.org/10.1016/j.conbuildmat.2015.07.141>
- [4] Nicolaidis, D., Kanellopoulos, A., Petrou, M., Savva, P. & Mina, A., Development of a new Ultra High Performance Fibre Reinforced Cementitious Composite (UHPFRCC) for impact and blast protection of structures. *Constr Build Mater*, **95**, pp. 667–674, 2015 October. <https://doi.org/10.1016/j.conbuildmat.2015.07.136>
- [5] Yoo, D.-Y., Kang, S.-T. & Yoon, Y.-S. Effect of fiber length and placement method on flexural behavior, tension-softening curve, and fiber distribution characteristics of UHPFRC. *Constr Build Mater*, **64**, pp. 67–81, 2014 August. <https://doi.org/10.1016/j.pii/S0950061814003249>
- [6] Lovichova, R., Fornusek, J., Mara, M., Kocova, M. & Rihova, Z., The fibre orientation influence in cementitious composite against extreme load resistance. *IOP Conf Ser Mater Sci Eng*, **307**(1), p. 012069, 2018 February. <https://doi.org/10.1088/1757-899X/307/1/012069>
- [7] Fornůsek, J. & Tvarog, M., Influence of casting direction on fracture energy of fiber-reinforced cement composites. *Key Eng Mater*, **594–595**, pp. 444–448, 2013 December. <https://doi.org/10.4028/www.scientific.net/kem.594-595.444>
- [8] Stiel, T., Karihaloo, B.L. & Fehling, E., Effect of casting direction on the mechanical properties of CARDIFRC. In *Proceedings of the International Symposium on Ultra High Performance Concrete*. pp. 481–493, 2004.

- [9] Lovichová, R., Takáčová, K., Künzel, K., Papež, V., Mára, M., Fornůsek, J., et al., Directed orientation of steel fibres in ultra-high-performance cementitious composite using the magnetic field. *WIT Trans Built Environ*, **196**, pp. 39–49, 2020.
- [10] Lovichova, R., Fornůsek, J., Soukupová, L. & Valentin, J.,. Ultrasound gel as suitable tool for simulation of the fibre orientation in the fibre reinforced concrete. In *54th International Conference on Experimental Stress Analysis*. Czech Society for Mechanics, pp. 1–4, 2016. <http://experimentalni-mechanika.cz/cs/konference/konference/2016>
- [11] Bažantová, Z., Kolář, K., Konvalinka, P. & Litoš, J., Multi-functional high-performance cement based composite. *Key Eng Mater*, **677**, pp. 53–56, 2016 January.